8

Egypt. J. Chem. **Vol. 64,** No. 1 pp. 75 - 84 (2021)

Molecular Modeling Analyses and Vibrational Characteristics for Nitromethane

Hend A. Ezzat[a] , Hanan Elhaes[b] , Ahmed Refaat[c,d] , Mohamed S. Abdel-Aal,[c] Medhat A. Ibrahim[c],*

[a] *Nano Technology Unit, Space Lab, Solar and Space Research Department, National Research Institute of Astronomy and Geophysics (Nano NRIAG), Helwan, Cairo, Egypt*
[b] *Physics Department, Faculty of Women for Arts, Science and Education, Ain Shams University, 11757 Cairo, Egypt.*
[c] *Molecular Spectroscopy and Modeling Unit, Spectroscopy Department, National Research Centre, 33 El-Bohouth Str. 12622 Dokki, Giza, Egypt*
[d] *Synchrotron-Light for Experimental Science and Applications in the Middle East (SESAME), Allan, JORDAN.*

Abstract

 Molecular modeling is considered as an effective tool for the evaluation of many physical as well as spectroscopic parameters. In this study semiempirical AM1, PM5, ab initio methods HF and MP2 as well as density functional methods VWN, B88LYP, B88PW91, B3PW91 and B3LYP were used to study nitromethane in its gas phase. The optimized structure, some physical parameters, and vibrational spectrum were calculated and discussed. The calculated optimized structure indicated that nitromethane (NM) belongs to the point group C2V. The obtained data indicated that quantum mixing gives results comparable to both ab initio method in accuracy and semiempirical method in computation time. It is concluded that for a small structure like NM, quantum mixing method provides reliable results in a short computation time. At B3LYP/6-31G(d,p) level, polar solvents showed changes in both HOMO/LUMO band gap energy and molecular electrostatic potential. This is an indication for the stability of NM in different chemical environments.

1. Introduction

Computational tools applied for molecular modeling could simulate several structures and reactions numerically, based in full or in part on the fundamental laws of physics [1-4]. Molecular modeling calculations continue to be a hot topic of research as they are available to study a large number of molecules and crystals, and interactions in many disciplines of science and technology [5-10]. The continuous advancements in computational methods have become part of the standard set of tools used in the development and evaluation of energetic materials [11]. NM continues to be a topic of many research activities since it is among the most considerable molecules as it shows a role in explosive materials and atmospheric pollution [12-14]. It is reported among the most recognized molecules in this class [15-17]. Furthermore, NM is also considered as an accurate and effective NMR probe for monitoring the basicity of oxide surfaces [14]. NM was also early reported as one of the well-known organic solvents [18-20]. From the spectroscopic point of view, the near-infrared overtone absorption spectrum of liquid-phase NM is reported [21]. It was proven experimentally that the rate of decomposition of the aliphatic nitro compounds in supercritical water depends on pressure/density at constant temperature [22]. It was also reported that saturated nitro compounds are relatively rare because they are not stable [23]. Based on these considerations, one can conclude that for such explosive structures, computational methods can provide useful physical, chemical and spectroscopic

data about these compounds [24]. Accordingly, NM has been the subject of numerous molecular modeling studies [25-31]. Additionally, kinetic modeling methods were also employed to study the properties of NM from different aspects, such as its oxidation [32], pyrolysis [33] and flames premixed with some gases [34], as well as studying the spatial distribution of its ground state precursors [35].

In the present work several models including AM1, PM5, VWN/DZVP, BLYP/DZVP, B88PW91/DZVP, B3PW91/6-31G(d,p), BLYP/DZVP and B3LYP/3-21G(d, p) were exploited to study both the crystal structure and vibrational spectrum of NM in its gas phase. Furthermore, two quantum mixing models; namely, B88PW91/DZVP and BLYP/DZVP were used and their results were compared with other models. Additionally, some physical parameters were calculated such as total dipole moment, polarizability, total energy and final heat of formation. To be helpful, since the available data in the literature are, to some extent, limited for this compound, the effect of solvents upon NM was calculated in terms of the molecular electrostatic potential (MESP) at B3LYP/6-31G(d,p).

2. Computational Details

Both B3LYP [36-38] and B3PW91 calculations were carried out using the Gaussian 09 [39] suite of programs at Spectroscopy Department, National Research Center, NRC, Egypt. Its geometries were fully optimized without imposing external symmetry constraints using both 3-21G(d,p) and 6-31G(d,p) basis sets. AM1 [40], PM5 [38], VWN, B88PW91 and BLYP were calculated on personal computer and were performed using quantum mechanical methods as implemented in the SCIGRESS software (by Fujitsu), also at Spectroscopy Department, National Research Center, NRC, Egypt. The geometries were optimized using DZVP basis set. The calculations were performed upon NM in gas phase. For ab initio methods, the frequencies were calculated beyond the harmonic approximation. Both HOMO/LUMO band gap energy and MESP were calculated for different solvents at B3LYP/6-31g(d,p). Seven solvents were studied; namely, water, Dimethyl Sulfoxide (DMSO), Acetonitrile, Methanol, Ethanol, Acetone and Dichloro-methane. The solvents were coded as S1 to S7, respectively.

3. Results and discussions

3.1. Crystal structure of nitromethane

Molecular modeling always provides valuable crystal structure data, particularly when the experimental data are limited and/or difficult to obtain. Furthermore, methods like ab initio exhibit reasonable accuracies coupled with computational efficiency, and for such reasons they have been adopted to study NM. NM is optimized and a stationary point is found. The optimized NM belongs to point group C2V. The results of calculated crystal structure are tabulated in Table 1 and the optimized structure is shown in Figure 1. C-H bond distances showed identical values around 1.10 Å irrespective of methods. Semiempirical calculated C-H bond distances are slightly longer than their ab initio calculated values. The calculated C-N bond distance is around 1.51 Å, with the exception that AM1 showed the lowest calculated value. Regarding the two bond distances of nitro group, both values of N-O are nearly the same with a bond distance value around 1.25 Å, while a small decrease was noticed in case of semiempirical calculations. On the other hand, a small increase was noticed in case of B3LYP/3-21G(d,p). From the data above, it is clear that for methyl group, the semiempirical calculated bond distances are longer than ab initio calculated ones, and the opposite is true in case of nitro group. Regarding bond angles, both O-N-O and C-H-C are higher in case of calculated ab initio methods. While C-N-O and H-C-N showed comparable values for both ab initio and semiempirical methods. The most interesting point is that the quantum mixing methods MM:B88PW91/DZVP and MM:BLYP/DZVP gave comparable results with those of ab initio. They have more advantages because they consume less computation time than ab initio calculations.

3.2. Calculated physical parameters

Beside the optimized geometry, there are some physical parameters that were calculated for the optimized NM such as total energy, total dipole moment and polarizability. These parameters are calculated and listed in Table 2.
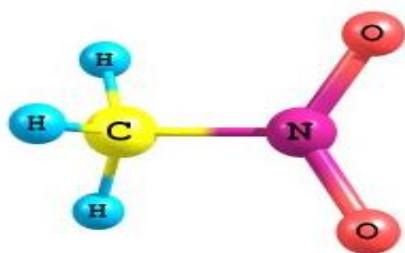
Fig. 1. B3LYP/6-31G(d,p) calculated optimized structure of nitromethane.

X= 3.4847 Y= -0.0016   Z= 0.0402

Dipole moment is defined as the first derivative of energy with respect to an electric field [2]. The calculated dipole moment can be expressed in terms of vector in three directions X, Y and Z. It is considered as being the measure of asymmetry in the NM charge distribution. The negative sign of the Y axis indicates that the dipole moment is pointing away from Y direction, while the positive sign of X and Z directions indicate that it points in both directions. The calculated total dipole moment is 3.4849 Debye. Another way to obtain information about the distribution of electrons in NM is polarizability. It depends on the second derivative of energy with respect to the electric field. Its results are obtained in a tensor triangular format such as (αxx, αxy, αyy, αxz, αyz, αzz). The approximate polarizability line gives the results of a crude polarizability estimate using over-state perturbation theory.

Table 1. The calculated bond distances in angstroms and bond angles in degrees for optimized NM at different models.

	Bond Lengths						Bond Angles			
	C-H$_5$	C-H$_6$	C-H$_7$	C-N	N-O$_3$	N-O$_4$	O-N-O	C-N-O	H-C-N	H-C-N
AM1	1.119	1.119	1.119	1.500	1.201	1.201	122.5	118.8	108.0	111.0
PM5	1.111	1.111	1.111	1.526	1.217	1.219	124.9	117.7	109.7	108.5
HF1	1.074	1.074	1.080	1.492	1.240	1.240	126.2	116.9	106.9	113.1
HF2	1.077	1.077	1.081	1.478	1.192	1.192	125.8	117.1	106.6	112.9
VW	1.099	1.100	1.096	1.520	1.252	1.252	125.8	117.6	108.2	109.5
PW1	1.099	1.099	1.095	1.508	1.243	1.243	125.9	117.5	108.3	109.3
PW2	1.092	1.088	1.088	1.492	1.112	1.212	126.0	116.9	108.0	110.5
PW3	1.090	1.090	1.090	1.520	1.299	1.280	120.0	119.9	109.5	109.5
BL1	1.099	1.100	1.097	1.520	1.252	1.252	125.8	117.7	108.3	109.5
BL2	1.099	1.099	1.097	1.519	1.252	1.253	125.7	117.8	108.5	109.4
BL3	1.089	1.084	1.084	1.518	1.277	1.278	127.1	113.1	105.2	111.1
BL4	1.088	1.088	1.092	1.498	1.227	1.227	125.9	117.1	106.9	112.8
MP2	1.083	1.083	1.086	1.486	1.241	1.241	125.77	117.09	107.14	112.65

HF1: HF/3-21G(d), HF2: HF/6-31G(d,p), VW: VWN/DZVP, PW1: B88PW91/DZVP, PW2: B3PW91/6-31G(d,p), PW3: MM B88PW91/DZVP, BL1: BLYP/DZVP, BL2: MM BLYP/DZVP, and BL3: B3LYP/3-21G(d,p), BL4: B3LYP/6-31G(d,p) and MP2: MP2/6-31G(d,p).

_____

Table 2. B3LYP/6-31G(d,p) calculated values of total energy in Hartree, total dipole moment in Debye and polarizability tensor for optimized
         nitromethane.

Parameter	Calculated value
Dipole moment vector	X= 3.4847 Y= -0.0016 Z= 0.0402
Total dipole moment	3.4849 Debye
Exact. polarizability	23.374 -0.060 30.719 -0.070 -0.004 14.000
Approx. polarizability	30.821 -0.300 85.329 -0.122 -0.002 17.300

Table 3. Some thermo-parameters, calculated at 298.15 K and 1.00 atm., pressure using B3LYP/6-31G(d,p).

Parameter	Hartree
SCF energy	243.6358 A.U.
E_o	-243.5883
E	-243.5838
H	-243.5828
G	-243.6158
Final heat of formation[*]	-11.5660 kcal/mol

* Calculated at PM3 semiempirical level.

Some thermo-parameters are calculated under normal conditions of temperature and pressure as mentioned in Table 3. The calculated parameters are obtained using the principal isotope for NM. Additionally, the parameters use the standard expression for an ideal gas in a canonical ensemble. The total energy of NM is calculated as 243.6358 A.U. which is the energy corresponding to the minimum structure of NM. Other thermo-parameter for NM is E_o, which is the sum of electronic and zero-point energies calculated as -243.5883 Hartree with an added zero-point correction amounting to 0.0485 Hartree. The sum of electronic and thermal energies, E, is calculated as -243.5838 Hartree. The sum of electronic and thermal enthalpies, H, is -243.6158 Hartree. Then the sum of electronic and thermal free energies, G, is -243.6158 Hartree. The last three parameters have corrections to their values estimated as 0.0530, 0.0539 and 0.0210 Hartree, respectively. These corrections to each energy of the NM are to account for the effects of molecular vibrations which persist even at 0 K. The calculated corrections are added to the total energy at higher temperature, rather than zero temperature. The final heat of formation is calculated to be -

11.5660 kcal/mol. It is the formation of NM relative to its elements in their standard state at 298.15 K.

3. 3. Calculated vibrational spectrum of NM

Energy calculations and geometry optimizations (crystal structure) ignore the vibrations in the NM molecule. This assumes that the nuclei are not in motion, while in reality the nuclei in NM are in motion. Furthermore, in equilibrium states, these vibrations are regular and predictable, therefore NM can be identified by its characteristic spectra [23]. The NM vibrations and their assignments are given in Table 4. It is worth mentioning that no negative frequencies are obtained, thus ensuring that the obtained structure is the optimal structure of NM. The assignment of this compound is aided by our previous work [4]. NM was optimized and the vibrational spectra were calculated at semiempirical, quantum mixing as well as ab initio levels of theory. The present computational study presents the NO_2 symmetric stretching as a characteristic band that possesses higher infrared intensity as compared to asymmetric stretching of the same functional group NO_2. This indicates a

_____

difference between the nitro group in both aromatic and saturated compounds on one hand, and in both liquid and gas phases on the other hand. The component of the dipole moment is largely found in the direction of the nitro group, and may be due to the existence of oxygen atoms which lead to a strong band of symmetric stretching in gas phase due to the high dipole moment of the nitro group.

It is well known that vibrational frequencies for species in complex environment can be computed by the combination of quantum calculations with classical molecular dynamics simulations [42-43]. Furthermore, the unsatisfactory state of these kinds of calculations was corrected by ab initio calculations. Regarding the calculated frequency with quantum mixing method (PW3 and BL2), one can observe the comparable results of these methods to the ab initio results.

Table 4. Unscaled calculated frequencies in cm^{-1} and band assignment for nitromethane as compared with experimental frequencies in gas phase.

AM1	PM5	HF1	HF2	VW	PW1	PW2	PW3	BL1	BL2	BL3	BL4	MP2	Assignment
62	40	139	15	288	62	20	333	63	74	46	29	38	τ CH$_3$
498	479	472	529	479	460	481	467	455	454	420	478	483	ρNO$_2$
1102	945	603	690	609	585	616	526	572	573	536	607	600	ρNO$_2$
733	624	667	743	629	627	672	580	611	611	596	662	672	δ_sNO$_2$
597	606	912	1051	862	888	945	686	863	864	824	929	945	ν_s CN
1102	1065	1153	1224	1045	1082	1109	861	1080	1077	1068	1111	1149	ρCH$_3$
1127	1068	1252	1263	1074	1097	1135	1046	1096	1094	1121	1137	1168	ρCH$_3$
1345	1187	1382	1557	1304	1363	1406	1072	1327	1326	1207	1410	1436	ν_sNO$_2$
1397	1201	1485	1591	1333	1382	1463	1191	1381	1380	1392	1442	1462	δ_s CH$_3$
1800	1298	1566	1605	1386	1436	1469	1360	1433	1432	1396	1475	1530	δ_a CH$_3$
2067	1454	1643	1688	1402	1448	1486	1433	1446	1445	1500	1489	1537	δ_a CH$_3$
3033	1704	1644	1879	1525	1586	1718	1437	1536	1534	1504	1680	1815	ν_a NO$_2$
3033	3061	3258	3247	3038	3033	3099	3108	3013	3020	3138	3091	3171	ν_s CH$_3$
3044	3085	3352	3346	3151	3134	3203	3216	3107	3113	3245	3188	3287	ν_a CH$_3$
3113	3090	3392	3381	3182	3166	3234	3219	3139	3146	3280	3220	3312	ν_a CH$_3$

HF1: HF/3-21G(d), HF2: HF/6-31G(d,p), VW: VWN/DZVP, PW1: B88PW91/DZVP, PW2: B3PW91/6-31G(d,p), PW3: MM B88PW91/DZVP, BL1: BLYP/DZVP, BL2: MM BLYP/DZVP, and BL3: B3LYP/3-21G(d,p), BL4: B3LYP/6-31G(d,p) and MP2: MP2/6-31G(d,p).

_____

3.4. Mapping Molecular Electrostatic Potential (MESP)

(a)

(b)
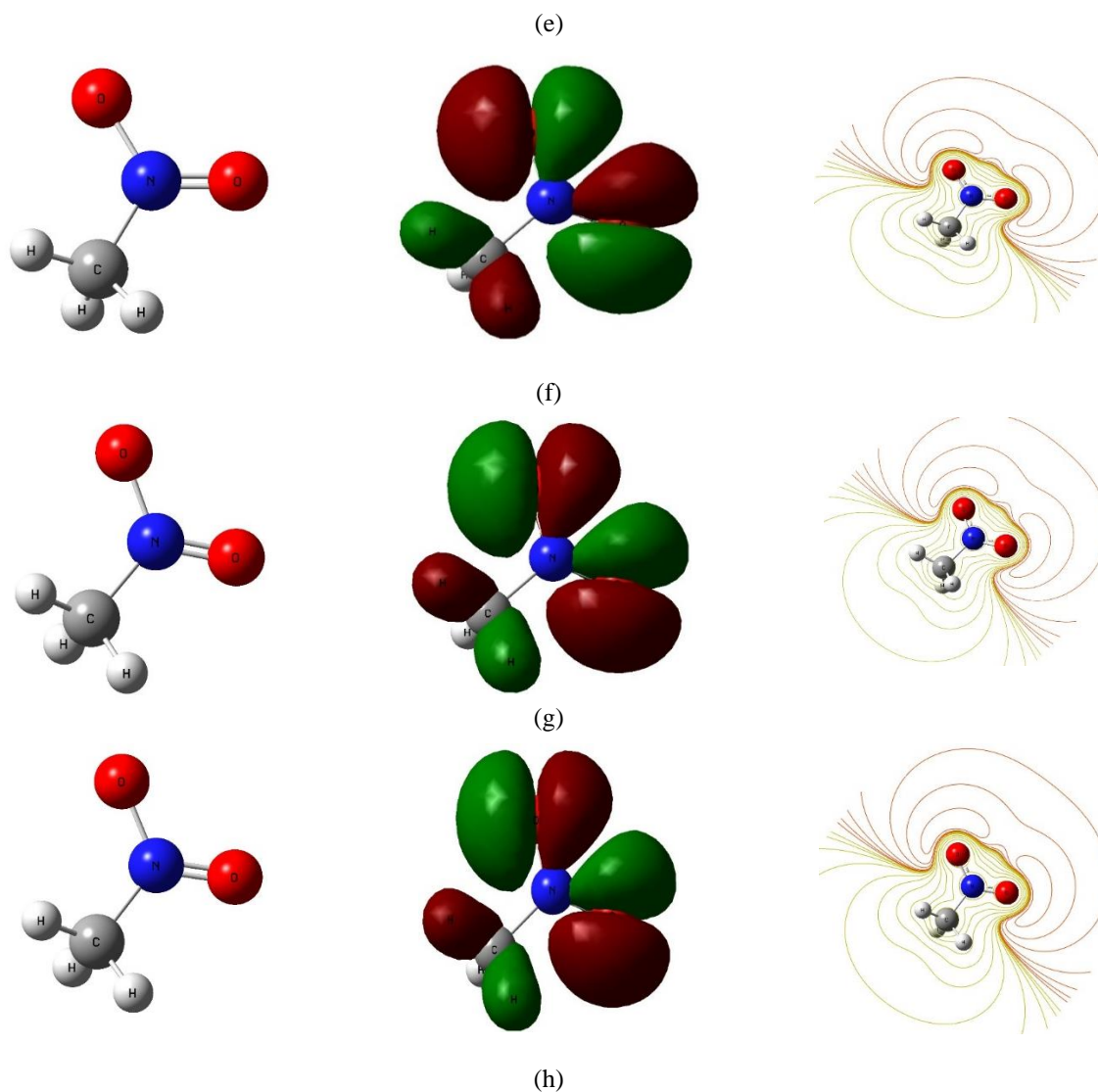

(c)

(d)

_____

(e)

(f)

(g)

(h)
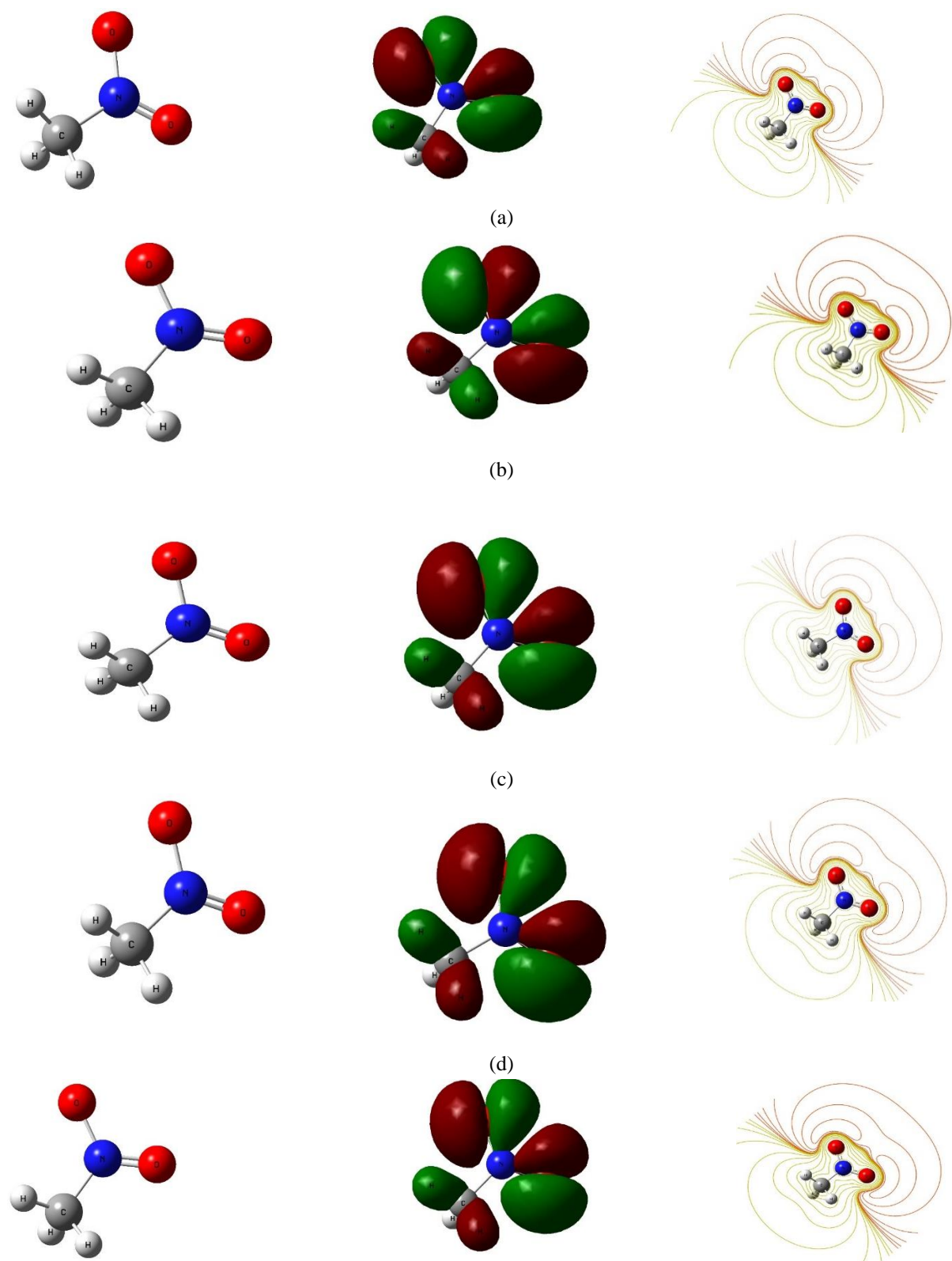
Fig 2. Models for the optimized HOMO-LUMO band gap energy and MESP for NM in different solvents (a) gas phase, (b) water, (c) DMSO, (d) acetonitrile, (e) methanol, (f) ethanol, (g) acetone, and (h) dichloro-methane.

Table 4. B3LYP/6-31G(d,p) calculated total dipole moment as Debye and HOMO/LUMO band gap energy as eV for NM in different solvents as compared with gas phase.

Solvent	TDM	ΔE
Water	4.1470	6.1381
DMSO	4.1385	6.1365
Acetonitrile	4.1324	6.1368
Methanol	4.1290	6.1368
Ethanol	4.1183	6.1368
Acetone	4.1109	6.1357
Dichloro-methane	4.0491	6.1343
Gas Phase	3.4849	6.1253

Table 4 presents the B3LYP/6-31G(d,p) calculated total dipole moment as Debye for the effect of solvents on NM as compared with gas phase NM. The studied solvents were water, DMSO, acetonitrile, methanol, ethanol, acetone and dichloro-methane respectively.

It is clear from the table that the total dipole moment is increased from 3.4849 (gas phase) to 4.1470 Debye (Water). Ongoing from water to dichloro-methane, the values of the total dipole moment almost did not change. As indicated in table 4, the band gap energy of NM is 6.1253 eV, but because of the effect of the solvents it became 6.1381 eV corresponding to water. It remained unchanged nearly for all the studied solvents, such that the increase in the band gap energy under the effect of solvents did not exceed 0.01 eV.

Figure 2 presents both the HOMO/LUMO orbitals and the mapping of the MESP for NM in gas phase as well as in the 6 respective solvents.

The MESP is not changed as a result of changing the solvents. This indicates that the active sites for NM are not changed as a result of interaction with environment containing polar solvents. This could be an indication for the suitability of NM as an organic solvent in many applications as its active sites are not changed with changing its chemical environment.

4.Conclusions

In this work, NM was subjected to computational modeling calculations. The crystal structure and some physical parameters like total dipole moment and polarizability, in addition to some thermo-chemical parameters like final heat of formation and energies are demonstrated. The vibrational spectra of gas phase NM were also obtained. This highlights the significance of the present model study presenting spectroscopic data for such a compound in its gas phase. The obtained spectroscopic data indicate that for a small system like NM, quantum mixing methods provide comparable data to those obtained with ab initio, and are fast like those obtained with semiempirical methods. Furthermore, ab initio calculations could be helpful for providing physical and thermo-parameters for NM in its gas phase. In terms of total

dipole moment, HOMO/LUMO band gap energy and MESP, strong organic solvents are not affecting the reactivity of NM. This could be an indication for its interaction with its surrounding environment whatever it is. Finally, molecular modeling is the most effective technique in the point that it provides researchers with physical data which are hardly obtained from other techniques.

2. References

[1] Hehre W.J., Radom L., Schleyer P.R. and Pople J.A., Ab initio Molecular Orbital Theory, John Wiley, New York (1986).

[2] Foresman J.B., Frisch A., Exploring chemistry with electronic structure methods, second ed., Gaussian Inc., Pittsburgh (1996).

[3] Ali G.W., Abdel-Fattah W.I., Elhaes H., Ibrahim M.A., Spectroscopic and modeling analyses of bimolecular structure of corn silk. Biointerface Research in Applied Chemistry, 9, 4581-4585 (2019).

[4] Abdelsalam H., Saroka V.A., Ali M., Teleb N.H., Elhaes H., Ibrahim M.A., Stability and electronic properties of edge functionalized silicene quantum dots: A first principles study. Physica E, 108, 339-346 (2019).

[5] Ibrahim M., Koglin E., Vibrational spectroscopic study of acetate group, Acta Chimica Slovenica, 51, 453-460 (2004).

[6] Ibrahim M., Mahmoud A.A., Computational Notes on the Reactivity of some Functional Groups, Journal of Computational and Theoretical Nanoscience, 6, 1523-1526 (2009).

[7] Bayoumy A.M., Badry R., Gaber H.A., Elbiomy S.A., El Gabaly S.G., Abd ElAziz M.S., Gouda S.M., Elhaes H., Yahia I.S., Zahran H.Y., Ibrahim M., Molecular modeling analyses for the effect of solvents on amino acids, Biointerface Research in Applied Chemistry, 9, 4379-4383 (2019).

[8] Ezzat H.A., Hegazy M.A., Nada N.A., Ibrahim M.A., Effect of Nano Metal Oxides on the Electronic Properties of Cellulose, Chitosan and Sodium Alginate, Biointerface Research in Applied Chemistry, 9, 4143-4149 (2019).

[9] Bayoumy A.M., Elhaes H., Osman O., Hussein T., Ibrahim M.A., Mapping Molecular Electrostatic Potential for Heme Interacting with Nano Metal Oxides, Biointerface Research in Applied Chemistry, 10, 5091-5095 (2020).

[10] Grenni P., Caracciolo A.B., Mariani L., Cardoni M., Riccucci C., Elhaes H., Ibrahim M.A., Effectiveness of a new green technology for metal removal from contaminated water, Microchemical Journal, 147, 1010-1020 (2019).

[11] Byrd E.F.C., Scuseria G.E., Chabalowski C.F., An ab Initio Study of Solid Nitromethane, HMX, RDX, and CL20: Successes and Failures of DFT, The Journal of Physical Chemistry B, 108, 13100-13106 (2004).

[12] Chen E.C.M., Welk N., Chen E.S., Wentworth W.E., Electron Affinity, Gas-Phase Acidity, Bond Dissociation Energy, and Negative Ion States of Nitromethane, The Journal of Physical Chemistry A, 103, 9072-9079 (1999).

[13] Zhang Y.X., Bauer S.H., Gas-phase decomposition mechanisms of C-NO2, N-NO2 energetic materials: Reevaluations, International journal of chemical kinetics, 31, 655-673 (1999).

[14] Bromly J.H., Barnes F.J., Mandyczewsky R., Edwards T.J., Haynes B.S., An experimental investigation of the mutually sensitised oxidation of nitric oxide and n-butane, In Symposium (International) on Combustion, 24, 899-907 (1992).

[15] Wodtke A.M., Hintsa E.J., Lee Y.T., Infrared multiphoton dissociation of three nitroalkanes, The Journal of Physical Chemistry, 90, 3549-3558 (1986).

[16] Vatsa R.K., Sarkar S.K., Mittal J.P., TEA CO2 laser-induced reaction of CH_3NO_2 with CF_2HCl: A mechanistic study, Journal of Chemical Sciences, 113, 333-342 (2001).

[17] Thomsen E.L., Nielsen O.J. and Egsgaard H., The reaction of nitromethane with hydrogen and deuterium atoms in the gas phase. A mechanistic study, Chemical physics letters, 215, 257-263 (1993).

[18] Enrique L., Louis C., Didier T., Monique L., Patrick G., Francueois F., Characterization of the Acid−Base Properties of Oxide Surfaces by 13C CP/MAS NMR Using Adsorption of Nitromethane, The Journal of Physical Chemistry B, 107, 4070-4073 (2003).

[19] Sirotkin V.A., Zinatullin A.N., Solomonov B.N., Faizullin D.A., Fedotov V.D., Calorimetric and FTIR-Spectroscopic Study of Solvent Effect on the State of Dry Solid Bovine Pancreatic A-Chymotrypsin Immersed in Anhydrous Organic Solvents, Biocatalysis, 41, 37-42 (2000).

[20] Kuriakose S., Vijayan K.K., Shaji S., Eappen S.M., Nair K.P.R., Rasheed T.M.A., CH overtone spectrum of nitromethane: a C_3V coupled oscillator analysis using local mode parameters. Spectrochimica Acta A, 60, 2283-2286 (2004).

[21] Anikeev V.I., Yermakova A., Semikolenov V.A., Goto M., Effect of supercritical water density on the rate constant of aliphatic nitrocompounds decomposition, The Journal of supercritical fluids, 33, 243-246 (2005).

[22] Smith B.C., Infrared Spectral Interpretation: A Systematic Approach, CRC Press LLC, Florida (1999).

[23] Foresman J.B., Ab initio Techniques in Chemistry: Interpretation and Visualization, Ed. M.L. Swift, T.J. Zielinski, What Every Chemist Should Know about Computing, ACS Books, Washington, D.C. (1996).

[24] Ibrahim M., Vibrational Spectroscopic Study of Gas Phase Nitromethane, Bulletin of the National Research Centre Egypt, 29, 100 (2004).

[25] Liu L.M., Car R., Selloni A., Dabbs D.M., Aksay I.A., Yetter R.A., Enhanced thermal decomposition of nitromethane on functionalized graphene sheets: ab initio molecular dynamics simulations, Journal of the American Chemical Society, 134, 19011-19016 (2012).

[26] Alper H.E., Abu-Awwad F., Politzer P., Molecular Dynamics Simulations of Liquid Nitromethane, The Journal of Physical Chemistry B, 103(44), 9738-9742 (1999).

[27] Feng S., Guo F., Yuan C., Cheng X., Li Z., Ab-initio molecular dynamics study on chemical decomposition reaction of α-HMX, Chemical Physics Letters, 748, 137394 (2020).

[28] Sorescu D.C., Rice B.M., Thompson D.L., Theoretical Studies of Solid Nitromethane, The Journal of Physical Chemistry B, 104, 8406-8419 (2000).

[29] Sorescu D.C., Rice B.M., Thompson D.L., Molecular Dynamics Simulations of Liquid Nitromethane, The Journal of Physical Chemistry A, 105(41), 9336-9346 (2001).

[30] Pruitt C.J.M., Albury R.M., Goebbert D.J., Photoelectron spectroscopy of nitromethane anion clusters, Chemical Physics Letters, 659, 142-147 (2016).

[31] Dryahina K., Polášek M., Španěl P., A selected ion flow tube, SIFT, study of the ion chemistry of H_3O^+, NO^+ and O^{2+}. ions with several nitroalkanes in the presence of water vapour, International Journal of Mass Spectrometry, 239, 57-65 (2004).

[32] Gao Z., Yang M., Tang C., Yang F., Yang K., Deng F., Huang Z., Measurements of the High Temperature Ignition Delay Times and Kinetic Modeling Study on Oxidation of Nitromethane, Combustion Science and Technology, 192, 313-334 (2020).

[33] Shrestha K.P., Vin N., Herbinet O., Seidel L., Battin-Leclerc F., Zeuch T., Mauss F., Insights into nitromethane combustion from detailed kinetic modeling – Pyrolysis experiments in jet-stirred and flow reactors, Fuel, 261, 116349 (2020).

[34] Zhang K., Li Y., Yuan T., Cai J., Glarborg P., Qi F., An experimental and kinetic modeling study of premixed nitromethane flames at low pressure, Proceedings of the Combustion Institute, 33, 407-414 (2011).

[35] Sheehe S.L., Jackson S.I., Spatial distribution of spectrally emitting species in a nitromethane–air diffusion flame and comparison with kinetic models, Combustion and Flame, 213, 184-193 (2020).

[36] Becke A.D., A new mixing of Hartree–Fock and local density functional theories, The Journal of chemical physics, 98, 1372-1377 (1993).

[37] Lee C., Yang W., Parr R.G., Development of the Colle-Salvetti correlation-energy formula into a functional of the electron density, Physical review B, 37, 785-789 (1988).

[38] Miehlich B., Savin A., Stoll H., Preuss H., Results obtained with the correlation energy density functionals of becke and Lee, Yang and Parr. Chemical Physics Letters, 157, 200-206 (1989).

[39] Frisch M.J., Trucks G.W., Schlegel H.B., Scuseria G.E., Robb M.A., Cheeseman J.R., Scalmani G., Barone V., Mennucci B., Petersson G.A., Nakatsuji H., Caricato M., Li X., Hratchian H.P., Izmaylov A.F., Bloino J., Zheng G., Sonnenberg J.L., Hada M., Ehara M., Toyota K., Fukuda R., Hasegawa J., Ishida M., Nakajima T., Honda Y., Kitao O., Nakai H., Vreven T., Montgomery, Jr. J.A., Peralta J.E., Ogliaro F., Bearpark M., Heyd J.J., Brothers E., Kudin K.N., Staroverov V.N., Keith T., Kobayashi R., Normand J., Raghavachari K., Rendell A., Burant J.C., Iyengar S.S., Tomasi J., Cossi M., Rega N., Millam J.M., Klene M., Knox J.E., Cross J.B., Bakken V., Adamo C., Jaramillo J., Gomperts R., Stratmann R.E., Yazyev O., Austin A.J., Cammi R., Pomelli C., Ochterski J.W., Martin R.L., Morokuma K., Zakrzewski V.G., Voth G.A., Salvador P., Dannenberg J.J., Dapprich S., Daniels A.D., Farkas Ö., Foresman J.B., Ortiz J.V., Cioslowski J. and Fox D.J., Gaussian 09, Revision D.01, Gaussian, Inc., Wallingford CT (2010).

[40] Dewar M.J.S., Zoebisch E.G., Healy E.F., Stewart J.J.P., Development and use of quantum mechanical molecular models. 76. AM1: a new general purpose quantum mechanical molecular model, Journal of the American Chemical Society, 107, 3902-3909 (1985).

[41] Stewart J.J.P., Optimization of parameters for semiempirical methods II Applications, Journal of computational chemistry,10, 209-220 (1989).

[42] Wang J., Boyd R.J. and Laaksonen A., A hybrid quantum mechanical force field molecular dynamics simulation of liquid methanol: Vibrational frequency shifts as a probe of the quantum mechanical/molecular mechanical coupling. J. Chem. Phys., 104, 7261-7269 (1996).

[43] Büschenfelde D.M.Z. and Staib A., Vibrational spectroscopy and molecular dynamics of solvated methanol tetramer and pentamer. Chem. Phys., 236(1-3), 253-261 (1998).